J Forensic Sci, May 2009, Vol. 54, No. 3
doi: 10.1111/j.1556-4029.2009.01037.x
Available online at: www.blackwell-synergy.com

TECHNICAL NOTE

Giampaolo Piga,[1] *M.Sc.; Tim J. U. Thompson,*[2] *Ph.D.; Assumpciò Malgosa,*[1] *Ph.D.; and Stefano Enzo,*[3] *M.Sc.*

The Potential of X-Ray Diffraction in the Analysis of Burned Remains from Forensic Contexts*

ABSTRACT: In view of the difficulties in extracting quantitative information from burned bone, we suggest a new and accurate method of determining the temperature and duration of burning of human remains in forensic contexts. Application of the powder X-ray diffraction approach to a sample of human bone and teeth allowed their microstructural behavior, as a function of temperature (200–1000°C) and duration of burning (0, 18, 36, and 60 min), to be predicted. The experimental results from the 57 human bone sections and 12 molar teeth determined that the growth of hydroxylapatite crystallites is a direct and predictable function of the applied temperature, which follows a nonlinear logistic relationship. This will allow the forensic investigator to acquire useful information about the equilibrium temperature brought about by the burning process and to suggest a reasonable duration of fire exposure.

KEYWORDS: forensic science, cremated remains, burned bones and teeth, hydroxylapatite, powder X-ray diffraction, forensic anthropology

The study of burned human remains is of considerable importance in forensic science, forensic anthropology, and crime scene investigation. An understanding of the changes that the body has undergone as a result of burning can provide significant information regarding the context and conditions of the burning event itself. Such crime scene information can include the temperature of the fire, the position of the fire, and the presence of accelerants. Unfortunately, the act of burning also causes a number of substantial changes to occur within the skeleton, which in turn can affect attempts to provide an identification of the deceased. Research has shown that both morphological and metric methods of anthropological assessment are affected (1,2), in addition to methods of dating (3) and stable isotopic analysis (4) (an analytical technique of increasing importance in the forensic field). Extracting this contextual information from the remains, in addition to determining the level of anthropological inaccuracy created by the burning event, is dependent upon being able to determine whether the skeletal remains have indeed been burned. Beyond this, one needs to be able to correlate the changes in the skeleton to this contextual information with confidence. Traditionally, a visual inspection of the remains has been used to suggest whether the bones have been subjected to fire (5–7), and beyond this, associations have been made between bone color and fracturing with fire temperature and presence of soft tissues (8,9). However, this can be complicated, and the links spurious. Furthermore, it has also been shown both experimentally and statistically that the most important changes in bone that can predict burning context involve changes within the skeletal microstructure (10). With all this in mind, it has been argued that a better and more reliable means of addressing these issues is with the powder X-ray diffraction (XRD) approach, possibly combined with other types of microscopic approaches (11), with a particular focus on the hydroxylapatite (HA) mineral phase, which is the main inorganic component of bones.

The HA phase is made of tiny micro- (or nano-) crystals with average size dimension around ca. 17 nm, that are subjected to growth changes when stimulated by the temperature of a fire. Broadly speaking, higher temperatures result in larger average sizes of HA nano-crystals, more ordered crystal structures and therefore sharper XRD peak profiles. These heat-induced crystal changes are akin to those resulting from standard bone diagenesis, and therefore we acknowledge that in the absence of important thermal effects, bone material decomposing for millions of years may undergo a similar crystal growth mechanism—which can also be detected and accurately measured with help of the XRD patterns (12–14).

The XRD technique was first applied to archaeological subjects in 1964 (15). Later Bonucci and Graziani (16) demonstrated that high temperatures of fire treatment induce a growth of the average crystallite size of HA, which can be appreciated relatively well from the line broadening/sharpening analysis of diffraction peaks. Since then, XRD has become a standard tool in anthropological work, although its adoption in forensic anthropology has been slow.

In the first critical study of its kind, Shipman et al. (17) investigated the microscopic morphology of various osteological materials and used XRD in order to assess whether specimens of unknown taphonomic history were burnt and the maximum temperature reached by those specimens. Like the previously cited studies, these investigations were based on the fact that heating of bone causes a sharpening of diffraction patterns, attributed to increased crystallite

[1]Unitat d'Antropologia, Department de Biologia Animal, Biologia Vegetal i Ecologia, Universitat Autònoma de Barcelona, Barcelona, Spain.
[2]School of Science & Technology, University of Teesside, Borough Road, Middlesbrough, UK.
[3]Department of Chemistry, University of Sassari, Sassari, Italy.

*Financial support provided by Sardinia Autonomous Region of Master and back project *TS160*.

Received 15 April 2008; and in revised form 4 Aug. 2008; accepted 9 Aug. 2008.

size and decreased lattice strain (i.e., increased organization of the crystal structure) of osteological phases. Rogers and Daniels (18) and other recent works (10,19) have also recorded key crystalline changes within the temperature range here investigated. The potential for XRD to associate crystal change to burning context is therefore not in doubt.

To further extend the validity of XRD methodologies that appear in the literature, we present a calibration for bones and teeth as a function of a range of temperatures of burning (200–1000°C), while simultaneously noting the effect of duration of burning (0, 18, 36, and 60 min). In practice, this would enable a more rounded account of the burning scenario to be realized. In fact, with this approach it will be possible to make an accurate estimation of both temperature and likely time duration of the firing process involved. This is not possible with current macroscopic approaches.

We have started our analysis with dry bone. First, we acknowledge that this may not entirely accurately mimic real-world scenarios; however, we argue that although the influence of soft tissues may affect the temperature/duration required to alter the bone microstructure to the level that we present, they would not alter the ability of XRD to associate these changes to a burning context. Second, it is unlikely that the presence of the organic component within the bone would alter the crystalline composition significantly from that in a dry bone (data to be published in the near future, but see also previous XRD studies augmented with thermo-gravimetry experiments). Bonhert et al. (20) observed that for total incineration of a body via cremation about 2 h are necessary at a constant temperature of 800°C, while for destruction of the fleshy parts about 50 min are believed to be needed. Thus, in the following study we have selected comparable burning times. Of course, it is not absolutely guaranteed that the ramp heating process applied in the laboratory furnace will accurately reproduce the heating process of a real fire. It should also be noted that a burning event may not cause complete change throughout the bone cortex; however, our XRD technique involves the grinding of bone samples, thereby assessing a volume-weighted average crystal size sampled over an at least "bimodal" distribution, which would reduce the influence of differences between the outer and inner regions of the bone.

Materials and Methods

We have used 57 human femoral fragments and 12 molar teeth for this experiment. The samples used for calibration were heat-treated with a heating rate of 20°C/min at selected temperatures (200–1000°C for 0, 18, 36, and 60 minutes) in air using a NEY muffle furnace. The specimens for X-ray investigations were powdered by manual grinding in an agate mortar.

The XRD patterns were recorded overnight using Bruker D8 (Bruker AXS GmbH, Karlsruhe, Germany), Philips PW-1050 (PANanalytical, Almelo, The Netherlands), Siemens D-500 (Siemens AG, Munich, Germany), and Rigaku D/MAX (Rigaku Corporation, Tokyo, Japan) diffractometers in the Bragg–Brentano geometry with CuKα radiation (λ = 1.54178 Å). The goniometer was equipped with a graphite monochromator in the diffracted beam and the patterns were collected with 0.05° of step size. The X-ray generator worked at a power of 40 kV and 30 mA and the resolution of the instruments (divergent and antiscatter slits of 0.5°) was determined using α-SiO_2 and α-Al_2O_3 standards free from the effect of reduced crystallite size and lattice defects. The powder patterns were collected in the angular range 15–120° in 2θ and were analyzed according to the Rietveld method (21), using the programme MAUD (22). This is an efficient approach that evaluates quantitatively the amount, structure, and microstructural parameters of mineralogical phases while keeping instrumental parameters into account. This is a necessary prerequisite in order to correctly distinguish the average crystallite size from the lattice disorder when using a peak broadening method such as this. This method may replace previous approaches that were adopted to study the bones based on an arbitrarily defined "index of crystallinity."

Results and Discussion

In Fig. 1, we report a pattern of XRD intensity from the untreated human femur sample, here studied as a function of the scattering angle 2θ. A full curve using the Rietveld fit has been calculated according to the 97 wt% contribution of the structure factors of HA (monoclinic, space group $P2_1/c$, refined lattice parameters a = 9.440, b = 18.898, c = 6.896 Å and β = 120.67°) and 3.0 wt% of calcite (trigonal, R-3c, a = 4.988, c = 17.070 Å) and has been added to the graph. As is usual in the Rietveld approach, the curve difference between calculated and experimental data points is shown at the bottom, while the sequence of bars indicate the expected peak positions for each phase. Examination of this feature is particularly useful in determining whether skeletal material has been burned or whether the changes are due to other taphonomic events (such as 23,24).

The quantitative Rietveld analysis points to the fact that HA is the main phase for bones. The structure of HA is reported as hexagonal with a space group of P63/mmc, but the monoclinic structure factor (25,26) was preferred here since it gave systematically better agreement factors with our results. The peak profiles of HA are very broad on account of the nanocrystalline condition of the material with very small average crystallite size and/or large lattice disorder. The average coherent diffraction domain calculated after separating strain from size effects according to the Rietveld approach is in the range between 168 and 170 Å.

Note that apart from the root mean square deviation problems, this result may be different from the figure normally obtained by applying the Scherrer equation (27) on the most intense peak. In fact, using this equation within the Rietveld approach for a modern bone, Michel et al. (28) determined an average crystallite size of 138 Å. The value may also be distinct from the average particle size that can be evaluated using SAXS data, as the latter may refer to a collection of agglomerated crystallites (10,29,30). Furthermore,

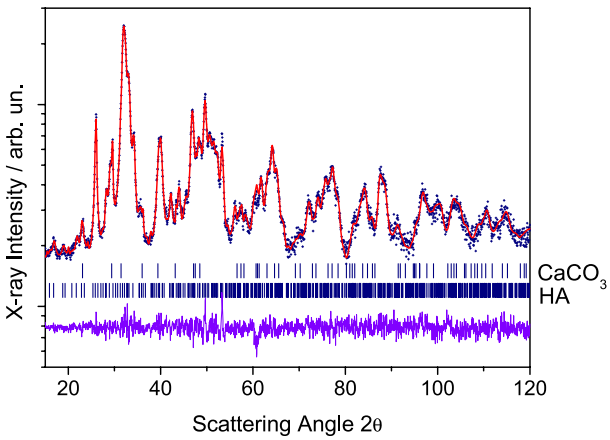

FIG. 1—*The XRD powder pattern of untreated femour fragment used as sample reference coming from the Grave yard ossuary of Sassari. Experiment are data points, full line is the Rietveld refinement on the basis of hydroxylapatite and calcite structure factors. The line at the bottom refers to the residuals, i.e., the difference between calculated and experimental square root intensities, which is indicative of the agreement obtained.*

it should be kept in mind that average values from transmission electron microscopy observations refer to a surface weighted mean (31), and thus may also differ from this work.

In Fig. 2, the XRD pattern and Rietveld fit of an untreated human tooth is reported. In comparison to Fig. 1, it can be seen that the peaks for calcite are absent. Moreover, the peaks for apatite appear sharper (on account of a larger average crystallite size of ca. 224 Å). Differences in microstructure are likely related to the different mechanical properties of apatite in teeth and bones, respectively.

The results of our investigation into the average crystallite size of the sample of femoral bone as a function of applied temperature (which is an equilibrium temperature of the furnace) and duration of burning are reported in Table 1 and given in Ångstrom (Å) units. For temperatures of 200°C to around 650°C (0 min) no significant growth of HA appears to be induced. Also, the burning times of 18, 36, and 60 min at these temperatures are not dramatically changing the microstructure, with only slight effects of grain growth, on account of a relative stability of the system. This is not so from 700°C (36, 60 min) to higher temperatures, where an effect of sudden growth appears evident and further distinguishable in the temperature range 750–850°C, where three separate trends for the growth processes can be evaluated. This is significant since this temperature range corresponds with the temperature of the average house fire (32). For specimens treated at temperatures higher than 850°C and for long burning times, the determination of the average crystallite size may be difficult to reproduce because of the upper resolution of instrument broadening. In fact, an upper limit of 1500 Å for crystal size determination is generally associated with this technique. This upper limit is a problem also experienced by other techniques (30).

The simplistic association between bony changes and temperature alone has been criticized previously, whereby it was argued that high temperature and low duration events may result in similar heat-induced changes to low temperature and high duration events (10). Our data confirms this assertion, as here a burning time of 60 min evidences an effect of crystallite growth that would be obtained at temperatures *c.* 100°C higher without any burning time.

The markedly different behavior for the specimens treated above 650°C is clearly seen in Fig. 3*a*, *b*, where symbols refer to the measured crystallite size values as a function of temperature treatment. For the sake of clarity, the results concerning the curve with 36 min of burning time are reported separately since they closely overlap the data of curve from 18 min exposure. Restricting our

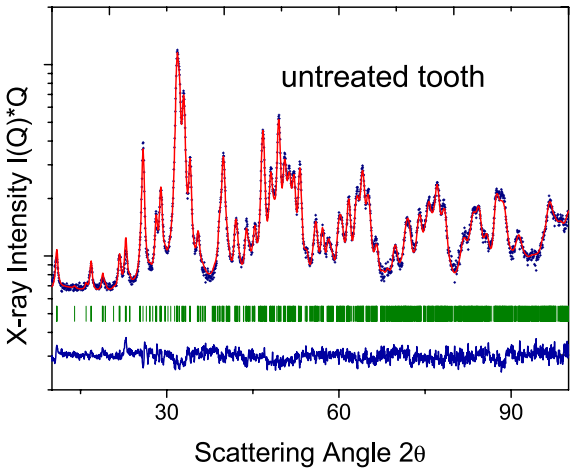

FIG. 2—*The XRD pattern (data points) and relevant Rietveld fit (full line) of an untreated tooth. From the quality of fit it is concluded that the tooth is made of pure apatite single-phase with average crystallite size of 224 Å, larger than the correspondent figure observed for human bones.*

TABLE 1—*Average crystallite size of the hydroxylapatite mineral phase (1 Å = 10^{-10} m).*

Temperature (°C)	0 min	18 min	36 min	60 min
Not burned	170			
200	175	175	175	175
300	180	184	186	188
400	195	203	204	205
500	202	202	205	210
600	204	226	230	256
650	213	240	250	258
700	229	294	463	486
750	268	611	712	800
775	350	836	880	920
800	432	1030	1160	1200
825	732	1120	1140	1254
850	923	1380	1450	1500
900	1351	>1500 (1616)	>1500 (1680)	>1500 (2621)
1000	>1500 (1569)	>1500 (2195)	>1500 (2600)	>1500 (2950)

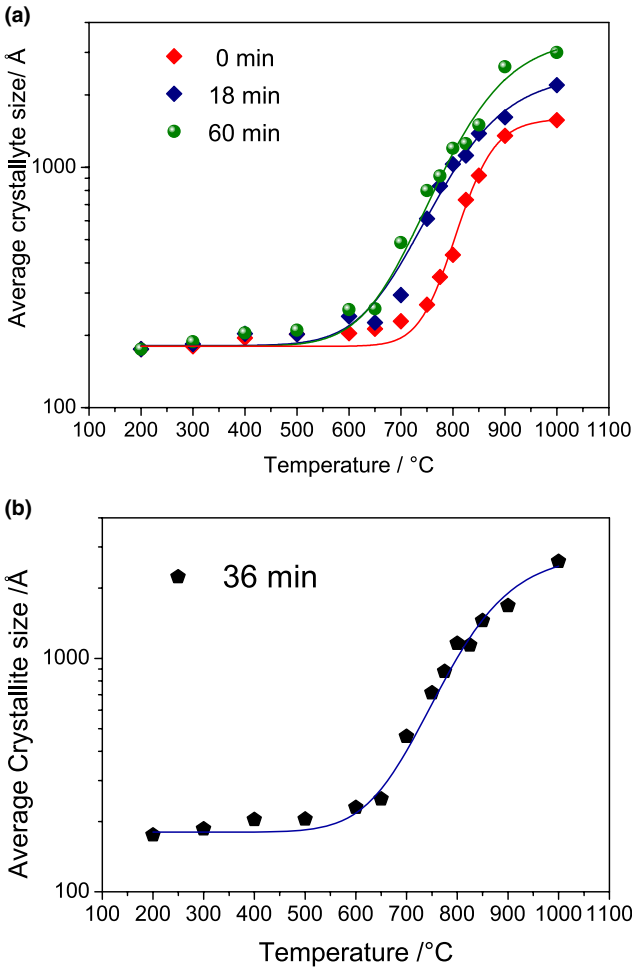

FIG. 3—*(a & b) The average crystallite size evolution for hydroxylapatite as a function of temperature treatment and residence times indicated. The experimental data from the Rietveld analysis have been fitted with sigmoid curves of logistic type which are typical of physico-chemical growth processes. The scatter of data and curves gives an idea of the uncertainty related to the determination of the temperature treatment for a bone of unknown provenance.*

attention to the specimens heated without any burning time, we can appreciate even with the logarithmic scale the rather sudden increase of the average crystallite size for temperatures around 750°C, in agreement with previous XRD observations.

The growth process seems to proceed up to 1000°C following a sigmoidal growth-type law typical of most reactions in a solid state. The following equation (full lines) was fit to the experimental data:

$$y = A_2 + (A_1 - A_2)/(1 + (x/x_0)^p)$$

The optimized parameters (presented in Table 2) have a precise physical meaning: A_1 value was actually fixed to the size dimension of HA for samples before any heat-induced growth; A_2 is the size limit reached at the end of the growth process; x_0 is the temperature relevant to the flex point of the logistic curves and p is a parameter for the growth rate, likely dependent on scanning rate, temperature, and duration of burning. Note that for the series with duration of 0 min the growth phenomenon is particularly sharp in the range 750–900 °C since p = 24, while for the other two curves the growth kinetics appears to occur in a more extended range from 600°C to 1000°C where the relevant p-values are quite close to 12.

It can be seen from Table 3 that the behavior and growth mechanism of teeth as a function of firing temperature (with 0 min of burning time) is similar to that observed in bones. This is a useful observation as it suggests that data collected from one hard tissue are applicable to the other. However, the final average values of HA microcrystallites at high temperature appear slightly reduced. This is of limited surprise since the enamel tooth crowns are known to fragment under firing in the temperature range between 700 and 750°C—presumably due to the high pressure exerted by water molecules trapped inside by the tooth enamel, which is of course made by highly compacted HA. Nonetheless, the data plotted confirm a logistic trend which was fitted again with the sigmoidal equation used previously. Of course, the A_1 parameter turns out to be close to the initial value for the average crystallite size of 224 Å, the A_2 figure was 994 Å, while the inflection point for the growth process X_o is located at 841 Å, with the p parameter of 17. These numerical parameters emphasize the similarities and differences between the behavior of teeth and bones as a function of temperature, which is reported for the sake of comparison in Fig. 4. As can be seen, the average size increases for the crystallites of HA are lower when compared to those observed for the HA of femoral bone, but the inflection point of the two sigmoidal curves appears to be practically the same.

TABLE 2—*The best-fit parameters of the four logistic curves represented in Fig. 3a and 3b.*

Parameters	0 min	18 min	36 min	60 min
A_1 (fixed)	180	180	180	180
A_2	1597	2420	2832	3528
X_0	845	844	855	860
p	24	12	12	12.46

At variance with duration of exposure, the three sigmoidal curves are all located around 850°C. The p parameter is related to the sharp behavior of the function.

TABLE 3—*The average crystallite size of HA phase of teeth as a function of temperature. Also, in this case the growth mechanism can be located at* c. *850°C.*

Temperature/°C	Average Cystallite Size
Not burned	224
200	227
300	228
400	230
500	233
600	245
700	293
750	345
800	400
850	659
900	827
1000	947

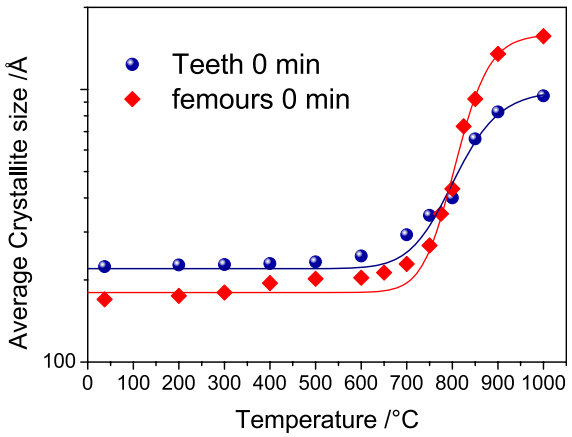

FIG. 4—*The comparison of the growth kinetics of hydroxylapatite crystallites as a function of temperature for teeth and bones at 0 min of residence time. Full lines are fit of experimental data according to the logistic function reported in the text. The characteristic temperature of the process (i.e. the inflection point of curves) is the same in the two cases while the sharpness and amplitude is larger for bones.*

We report in Fig. 5 a selected portion of the patterns from between 30° to 39° in 2θ from the burning of the femoral specimens at temperatures of 700, 775, 800, 825, 850, 900, and 1000°C, respectively. Figure 5 shows the disappearance of the calcite and

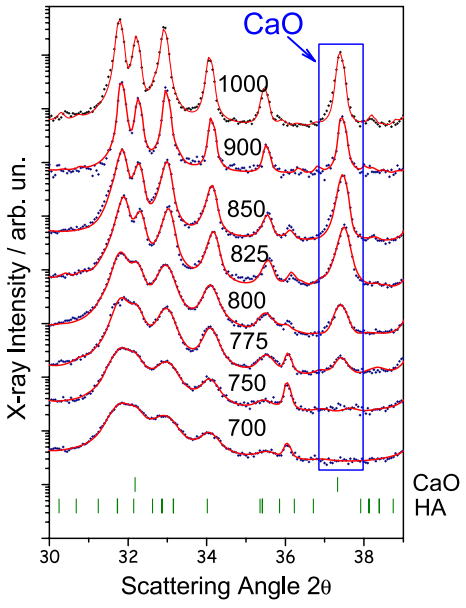

FIG. 5—*A selected range of the XRD patterns of sample bone treated at the indicated temperatures. It is evident the progressive peak sharpening of hydroxylapatite as a function of the indicated temperatures, simultaneous to the appearance of CaO phase following the decarbonization reaction which starts at 775°C.*

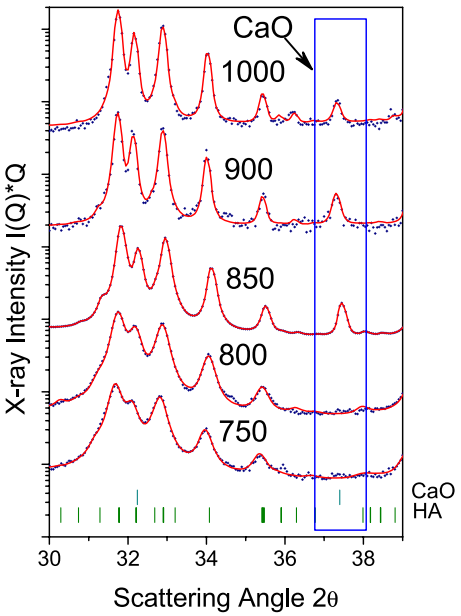

FIG. 6—*A selected portion of the XRD patterns of teeth treated at the quoted temperatures (data points) with the correspondent Rietveld fit (full lines). The appearance of the CaO cubic phase is perceived after treatment at 850°C. The fraction of CaO with respect to hydroxylapatite is lower than for the case of bones.*

the simultaneous appearance of calcium oxide. As can be seen, the peak of calcium oxide occurring at $2\theta = 37.5°$ starts to appear at 775°C, becoming more evident at 800°C and increasing with temperature until 1000°C where this phase reaches its maximum amount. Again, this is significant as it suggests another mechanism for differentiating burned from non-burned forensic specimens.

Results are somewhat different with the dental samples. First, no important contribution of calcite is observed in the teeth patterns. As can be seen in Fig. 6, during the process of apatite growth induced by thermal treatment, the calcium oxide peak starts to be visible in the teeth at *c.* 850°C, while in the bones the calcium oxide peak was evaluated after burning at 775°C. In addition to this, the amount of calcium oxide decomposed appears to be lower (*c.* 1.0 wt%) in the case of teeth, where a concentration value of 7.0 wt% was determined. It can also be seen that at 1000°C apatite can also decompose a fraction (10.0 wt%) of the $Ca_9MgNaP_7O_{28}$ phase, which turns out to be trigonal, with lattice parameter $a = 10.355$; $c = 37.09$ Å (33).

Conclusions

A means to estimate the temperature and duration of a forensic burning event, focussing on the microscopic changes in bone and teeth and using powder XRD has been developed. The technique is particularly appropriate for events within the temperature range 200–1000°C for a variety of burning times. This range includes most forensic scenarios, although it should also be noted that this range would include most archaeological scenarios too and that this methodology would be appropriate for those contexts.

The growth process undergone by the HA crystallites in the mineralogical phase of the femoral samples follows a logarithmic sigmoid trend with a characteristic temperature around 850°C, as was determined with the four duration of burning times adopted here. This can be used not only to determine whether hard tissues have been burned, but also to suggest the temperature and duration of that burning event. In the thermal treatment of 0 min, the growth rate parameter p seems to be higher than in the results from increased periods of burning. Thermal treatments at a given temperature for 60 min demonstrate the equivalent growth effects for 0 min of burning but at 100°C higher.

In the case of teeth, the growth phenomena induced by firing are again described with a logistic type function with a characteristic temperature of 841°C, very close to that of bones, in spite of typical fragmentation induced in the temperature range 700–750°C. However, the average crystallite size of HA in untreated teeth (224 Å) is significantly larger than in untreated skeletal bones (*c.* 170 Å), respectively. Alternatively, the average size of HA crystallites from burning above 900°C is larger in bones than teeth. This suggests that the two types of natural bioapatite need to be compared to their specific calibration curves when the precise estimation of the temperature of a fire is desired, and that one curve for all hard tissues is not advised.

Acknowledgments

The authors thank Prof. Vittorio Mazzarello (University of Sassari) for supplying the osseous materials employed in this study. Thanks are also due to: Dr. Ignasi Galtès (Universitat Autònoma de Barcelona) for helpful discussions concerning the forensic applications.

References

1. Thompson TJU. The assessment of sex in cremated individuals: some cautionary notes. Can Soc J Forensic Sci 2002;35:49–56.
2. Thompson TJU. Recent advances in the study of burned bone and their implications for forensic anthropology. Forensic Sci Int 2004;146S: S203–5.
3. Olsen J, Heinemeier J, Bennike P, Krause C, Hornstrup KM, Thrane H. Characterisation and blind testing of radiocarbon dating of cremated bone. J Archaeol Sci 2008;35:791–800.
4. Munro LE, Longstaffe FJ, White CD. Burning and boiling of modern deer bone: effects on crystallinity and oxygen isotope composition of bioapatite phosphate. Palaeogeogr Palaeoclimatol Palaeoecol 2007; 249:90–102.
5. Holck P. Cremated bones: a medical and anthropological study of an archeological material on cremation burials [PhD thesis]. Oslo: Anatomical Institute, University of Oslo, 1986.
6. Eckert WG, James S, Katchis S. Investigation of cremations and severely burned bodies. Am J Forensic Med Pathol 1988;9:188–200.
7. Etxeberria F. Aspectos macroscópicos del hueso sometido al fuego. Revisión de las cremaciones descritas en el País Vasco desde la Arqueología. Munibe 1994;46:111–6.
8. McKinley JI. The analysis of cremated bone. In: Cox M, Mays S, editors. Human osteology: in archaeology and forensic science. London, GB: Greenwich Medical Media Ltd, 2000;403–21.
9. Mayne Correia PM. Fire modification of bone: a review of the literature. In: Haglund WD, Sorg MH, editors. Forensic taphonomy: the post-mortem fate of human remains. USA: CRC Press, Inc., 1997;275–93.
10. Thompson TJU. Heat-induced dimensional changes in bone and their consequences for forensic anthropology. J Forensic Sci 2005;50(5): 1008–15.
11. Holden JL, Phakey PP, Clement JG. Scanning electron microscope observations of heat-treated human bone. Forensic Sci Int 1995;74: 29–45.
12. Bartsiokas A, Middleton MP. Characterization and dating of recent and fossil bone by X-ray diffraction. J Archaeol Sci 1992;19:63–72.
13. Person A, Bocherens H, Saliège JF, Paris F, Zeitoun V, Gérard M. Early diagenetic evolution of bone phosphate: an x-ray diffractometry analysis. J Archaeol Sci 1995;22:211–21.
14. Farlow JO, Argast A. Preservation of fossil bone from the Pipe Creek Sinkhole (Late Neogene, Grant County, Indiana U.S.A). J Paleont Soc Korea 2006;22(1):51–75.
15. Perinet G. Determination par diffraction X de la temperature de cuisson d'un ossement calcinè. Application au materiel prehistorique. Comptes Rendus d'Academie des Sciences, Paris (Series D) 1964;258:4115–6.

16. Bonucci E, Graziani G. Comparative thermogravimetric X-ray diffraction and electron microscope investigations of burnt bones from recent, ancient and prehistoric age. Atti della accademia Nazionale dei Lincei, Rendiconti, classe di scienze fisiche, matematiche e naturali 1975;59:517–32.
17. Shipman P, Foster G, Schoeninger M. Burnt bones and teeth: an experimental study of color, morphology, crystal structure and shrinkage. J Archaeol Sci 1984;11:307–25.
18. Rogers KD, Daniels P. An x-ray diffraction study of the effects of heat treatment on bone mineral microstructure. Biomaterials 2002;23:2577–85.
19. Kalsbeek N, Richter J. Preservation of burned bones: an investigation of the effects of temperature and pH on hardness. Stud Conserv 2006;5:123–37.
20. Bohnert M, Rost T, Pollak S. The degree of destruction of human bodies in relation to the duration of the fire. Forensic Sci Int 1998;95:11–21.
21. Rietveld HM. Line profiles of neutron powder-diffraction peaks for structure refinement. Acta Crystallogr 1967;22:151–2.
22. Lutterotti L, Ceccato R, Dal Maschio R, Pagani E. Quantitative analysis of silicate glass in ceramic materials by the Rietveld method. Mater Sci Forum 1998;281:87–92.
23. Sillen A, Hoering T. Chemical characterization of burnt bones from Swartkrans. In: Brain CK, editor. Swartkrans: a cave's chronicle of early man. Cape: Transvaal Museum Monograph #8, 1993;243–9.
24. Roberts SJ, Smith CI, Millard A, Collins MJ. The taphonomy of cooked bone: characterizing boiling and its physio-chemical effects. Archaeometry 2002;44:485–94.
25. Elliott JC, Mackie PE, Young RA. Monoclinic hydroxyapatite. Science 1973;180(4090):1055–7.
26. Ikoma T, Yamazaki A, Nakamura S, Akao M. Preparation and structure refinement of monoclinic hydroxyapatite. J Solid State Chem 1999; 144(5):272–6.
27. Scherrer P. Bestimmung der Größe und der inneren Struktur von Kolloidteilchen mittels Röntgenstrahlen. Nachrichten von der Gesellschaft der Wissenschaften zu Göttingen, Mathematisch-Physikalische Klasse 1918;2:98.
28. Michel V, Ildefonse Ph, Morin G. Assessment of archaeological bone and dentine preservation from Lazaret Cave (Middle Pleistocene) in France. Palaeogeogr Palaeoclimatol Palaeoecol 1996;126:109–19.
29. Guinier A. X-ray diffraction in crystals, imperfect crystals, and amorphous bodies. New York: Dover Publications Inc., 1963.
30. Hiller JC, Thompson TJU, Evison MP, Chamberlain AT, Wess TJ. Bone mineral change during experimental heating: an X-ray scattering investigation. Biomaterials 2003;24:5091–7.
31. Matyi RJ, Schwartz LH, Butt JB. Particle size, particle size distribution, and related measurements of supported metal catalysts. Catal Rev: Sci Eng 1987;29(1):41–9.
32. Richards NF. Fire investigation—destruction of corpses. Med Sci Law 1977;17:79–82.
33. Morozov VA, Presnyakov IA, Belik AA, Khasanov SS, Lazoryak BI. Crystal structures of triple calcium, magnesium and alkali metal phosphates $Ca_9MgM(PO_4)_7$ (M = Li, Na, K). Kristallografiya 1997;42:798–803.

Additional information and reprint requests:
Tim Thompson, M.Sc., Ph.D.
School of Science & Technology
University of Teesside
Borough Road
Middlesbrough
Cleveland TS1 3BA
United Kingdom
E-mail: t.thompson@tees.ac.uk